Available online at www.sciencedirect.com
ScienceDirect
Energy Reports 8 (2022) 1515–1529
www.elsevier.com/locate/egyr

TMREES22-Fr, EURACA, 09 to 11 May 2022, Metz-Grand Est, France

The effect of complex load on the reliable operation of solar photovoltaic and wind power stations integrated into energy systems and into off-grid energy areas

Pavel V. Ilyushin[a], Olga V. Shepovalova[b,*], Sergey P. Filippov[a], Anton A. Nekrasov[b]

[a] *Energy Research Institute of the Russian Academy of Sciences (ERI RAS), Nagornaya st. 31/2, Moscow, 117186, Russia*
[b] *Federal Scientific Agroengineering Center VIM (FSAC VIM), 1-st Institutskiy proezd, 5, Moscow, 109428, Russia*

Received 16 August 2022; accepted 17 August 2022
Available online xxxx

Abstract

A mass renewable power stations commissioning, first of all solar photovoltaic stations (SPVS) and wind power stations (WPS) shall be associated with the properly implemented complex load modeling while calculating their electric operation modes. This article deals with the basic failures of standard algorithm of SPVS and WPS invertors/converters, Fault Ride Through (FRT), that has to reduce the active power output and to increase that of reactive power, in case of voltage drop. In order to prevent outages of SPVS and WPS equipment during emergency disturbances, the trip set points of SPVS and WPS inventors/converters shall be adjusted to those of the adjacent power network protective relay. In this article, an approach to selecting methods for complex loads modeling, in industrial energy areas, has been developed. A method for calculating the value of critical voltage across the load bars has been considered, and the relevancy to apply the dynamic scale model of electric motor has been substantiated. The specific aspects of the voltage-dependent and frequency-dependent load static characteristics employment, in calculations of electromechanical transient processes, have been analyzed. Recommendations on representing electric motors integrated into complex load circuits, in various software packages designed for operation modes calculations, have been stipulated. Various methods making it possible to take account of electromagnetic transient processes, in rotors of asynchronous motors, have been described. A proper account of complex loads enables to ensure reliable functioning of SPVS and WPS integrated into energy systems and operating in isolated energy areas avoiding their outages including those disturbances in power supply of power consuming equipment of industrial areas.

Peer-review under responsibility of the scientific committee of the TMREES22-Fr, EURACA, 2022.

Keywords: Solar photovoltaic stations; Wind power stations; Complex load; Undervolage; Synchronous and asynchronous motors; Electromechanical transient process; Load modeling

1. Introduction

In recent years, there is a distinct global trend of the step-by-step reduction of the share of conventional energy sources (such as coal, peat, oil, natural gas) that is accompanied by mass-scale building renewable power stations

* Corresponding author.
E-mail address: shepovalovaolga@mail.ru (O.V. Shepovalova).

https://doi.org/10.1016/j.egyr.2022.08.218

Peer-review under responsibility of the scientific committee of the TMREES22-Fr, EURACA, 2022.

(RPS) The major role of the new generating capacities put into operation, in the field of electric industry belongs to the wind and solar power (Zeng et al. 2016 [1]; Eroshenko et al. 2016 [2]; Izmailov et al. 2019 [3]). This is being done for the sake of the carbon-neutrality concept implementation considering the demands of population for all necessary energy forms in the required amounts and at an acceptable price. Besides, requirements of reliability and accessibility of energy provision have to be observed (Buchholz and Styczynski, 2014 [4]; Papkov et al. 2015 [5]; Ilyushin et al. 2021a [6]; Rylov et al. 2021 [7]).

RPSs, first of all solar photovoltaic stations (SPVS) and wind power stations (WPS) are put into operation, in a mass-scale, which requires correctly performed modeling impedance loads, while calculating operating conditions of electric power circuits. The reason is that the aggregate capacity of the RPSs and other generating equipment is well comparable to that of loads, in both island and stand-alone modes. One more reason is rather low value of their interaction impedance. Alarm disturbances associated with undervoltages followed by electric motors automatic running often lead to the shutdowns of RPSs and to the deficiency of active power.

Many years' experience has shown that particular energy areas operating in parallel with the energy system may be separated from it into the island mode (isolated network operation) for various reasons. Most frequently it happens as a result of OHL emergency de-energizing, during repair and maintenance works on the power network. Such situations do not rarely occur. That is why they have to be studied in detail with the aim to ensure reliable functioning of RPSs and other power generating plants (PGP) thus providing guaranteed energy supply to consumers as long as this energy area is not synchronized to the energy system. Apart from PGPs on the basis of renewable energy sources, turbine-engined (TEP), gas piston (GPP), diesel generating (DGP) and other power generating plants playing the role of the mains frequency generator may be in operation, in energy areas (Zimba et al. 2017 [8]; Singh et al. 2017 [9]; Ilyushin et al. 2021b [10]; Shepovalova, 2019 [11]; Shepovalova, 2017 [12]; Strebkov et al. 2019 [13]; Khimenko et al. (2020) [14]).

In isolated energy areas, emergency processes characterized by active power deficiency proceed in much more heavy-duty conditions compared to their operation in parallel with the energy system (Li et al. 2017 [15]; Tina et al. 2018 [16]; Eroshenko and Ilyushin, 2018 [17]; Ufa RA et al. (2022) [18]).

The major share of the RPSs, excluding large wind-power and solar fields, are integrated into the networks of medium voltage 6 kV to 35 kV (capacity 5 MW to 10 MW per one line) and of high voltage 110 kV to 220 kV (capacity 25 MW to 100 MW per one line). In accordance with this concept, the major part of small and medium-size industrial enterprises having similar power consumption are connected to the medium and high voltage networks.

The principal difference between industrial enterprises and residential energy consumers (population and consumers considered equivalent to this group) is their power consumption structure. In industrial enterprises, the major part of electric energy (from 60 % to 95 %) is consumed by asynchronous (AEM) and synchronous (SEM) motors which is determined by the specifics of the technological process. Typically, direct connection electric motors are applied since they are much cheaper compared to those of inverter-type (Gurevich and Libova, 2008 [19]; Gurevich and Kabikov, 2005 [20]).

Taking into account that RPSs are distributed over the territories, the aggregate capacities of PGP and electric motors are nearly of the same order of magnitude, and that interdependent electric resistances are small, motor load parameters may substantially affect EMTP character and parameters, in distribution networks of medium and high voltage.

The aim of this article is to analyze the specifics of load impedance modeling while calculating operating mods in energy systems and isolated energy areas with SPVSs and WPSs. The principal task was an adequate account of loads, in the design process, with the aim of ensuring reliable functioning of SPVSs and WPSs and energy supply to electric receivers, in industrial energy areas, thus minimizing possible damage.

2. Methodology

2.1. Effect of electric motor loads on the operation conditions of SPVSs and WPSs

In regulation documents of various countries, the response of PGPs of all types including SPVSs and WPSs ones on the standard disturbances in energy systems is subject to the specification. The specified requirements are normally stipulated in the corresponding grid codes that do not leave place for shutting-off SPVSs and WPSs due to the short-term undervoltage of the specified amplitude and duration.

In accordance with these requirements, standard algorithm 'Fault Ride Through' (FRT) has to be adhered to, in SPVS and WPS inverters/converters, ensuring fast reduction of active power output and reactive power boost output into the adjacent network, in undervoltage conditions.

If the preset points of inverters/converters protection are adjusted to those of PR devices, in the adjacent network, SC occurred in the network adjacent to SPVS and WPS will be quickly eliminated with the help of PR devices integrated into the electric network components. In case of undervoltage, FRT algorithm activates in all SPVS and WPS inverters/converters thus contributing to fast recovering the parameters of operating mode. Outage of SPVS and WPS will not occur in this situation, and the initial value of the output active power will be restored, in the network, at the rate corresponding to the preset time constant (Mokryani et al. 2017 [21]; Shushpanov, 2021 [22]).

However, in case that the time of SC remedy by PR devices, in the distributionoĭ network adjacent to the SPVSs and WPSs, is as high as 0.8 s (i.e. exceeds 0.5 s), for instance, due to the activation of the main protection equipment having the time delay function or of the back-up protection the transient process will have the form shown in Fig. 1.

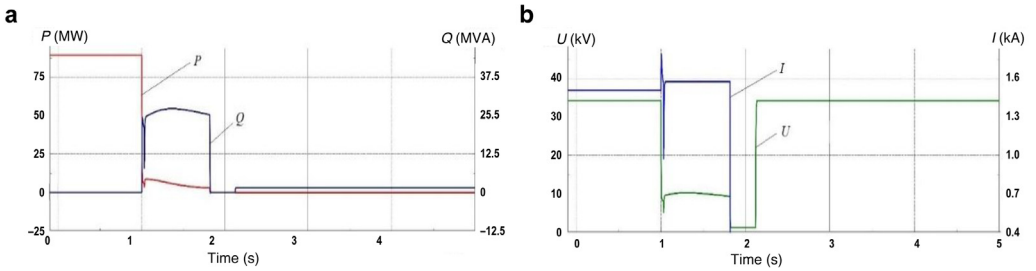

Fig. 1. Transient process for 0.8 s long SC in the network adjacent to SPVS or WPS: (a) active and reactive output power of SPVS or WPS, (b) voltagee and current flowing from the SPVS or WPS towards SC location.

It is clear from Fig. 1 that, during a long SC in the adjacent network, its operation parameters exceed the limits of the tolerance range. In this case, FRT algorithm activates, in WPP inverters/converters, but they get shut-down due to the safety trip of these inverters/converters. Such transient processes make the operating situation still worse because the deficit of active capacity takes place equal to the output power of particular SPVS or WPS, in pre-fault conditions (Gurevich et al. 1990 [23]). Therefore, relevant emergency prevention operations have to be provided in order to compensate this deficit. It can be done either by sharp increasing the active power output by PGP on non-renewable energy sources or by switching-off a certain part of industrial loads which will result in material damage and defective products.

Results of EMTP calculations for industrial energy areas comprising SPVSs and WPSs show that, in case of 0.4 s long SC, duration of undervoltage conditions on the output terminals of SPVSs and WPSs will be nearly twice as long as that of SC, i.e. 0.8 s. It is the consequence of the electric motors automatic starting process when they consume many folds larger reactive power to recover the rated slip value s_r.

Therefore, in case of a three-phase SC in industrial energy area, the time of voltage recovery to the level $0.9U_N$ is about twice as large as that of SC duration. When the time of SC recovery exceeds 1 s (activation of backup protection) electric motor automatic starting becomes either too long or principally impossible in which case all SPVSs and WPSs will be shut-off by the protection systems of inverters/converters.

In the course voltage recovering after SC elimination, reactive power surge occurs, in the OHLs connecting the energy area with the energy system, or in the SPVSs and WPSs (other PGPs) operating in the island mode due to AEM automatic starting. This leads to deep undervoltages, in nods, and to the active power surge, in the end of AEM automatic starting. That is why, in industrial energy areas, PR equipment redesign is required in the network adjacent to the SPVSs and WPSs in order to reduce SC recovery time to a value of 0.1 to 0.2 s. In these circumstances, all inverters/converters in SPVSs and WPSs will stay in operation thus avoiding emergency power deficit requiring certain compensation activities with the use of additional PGPs (Raza et al. 2017 [24]; Ruchika et al. 2017 [25]; Ramadan et al. 2017 [26]).

EMTP calculations were carried out that made it possible to conclude that particular regard has to be payed to the load modeling methods in order to ensure reliable SPVSs and WPSs operation as a part of an energy system or isolated energy areas with industrial enterprises. The accuracy of electric motor operation modeling defines that of eru calculation results and, therefore, is principally important in terms of selecting appropriate design concepts

concerning PR devices operation algorithms and adjustment parameters, in adjacent networks, as well as the settings of protection devices of inverters/converters of SPVSs and WPSs (Singh and Sharma, 2017 [27]; Mehigan et al. 2018 [28]).

Let us consider the general aspects of the electric motor loads modeling, in EMTP calculations, in greater detail.

2.2. General problems of electric motor load modeling

The basic type of motor loads, in industrial energy areas, determining the character and parameters of the transient processes is AEM. The reason is that the power consumption of AEM changes considerably in time, in post-emergency operation conditions, which is the consequence of the automatic starting processes.

SEMs are in practical use in industrial energy areas, as well, but their number and aggregate capacity are normally insignificant. SEM models has to be taken in consideration in calculation models, for the energy area, when either their share is sufficiently high, in the total load, or their unit capacity is sufficiently large in which case their individual characteristics have to be used and particular types of the driven mechanisms have to be taken into account.

The heaviest possible consequence of an emergency disturbance is the voltage collapse that often develops, in industrial energy areas. Voltage collapse may occur if a large number of AEMs and SEMs change their state during short-term undervoltage resulting in further voltage reduction. In these conditions, other AEMs and SEMs that have operated with the rotation velocities close to their normal values may easily change their state, as well. During voltage collapse, stationary-state voltage values, in the network nods, may be as low as 0.1 U_N to 0.4 U_N in which case electric motors that have stopped will be switched-off by their PR equipment.

At the stage of designing, various software packages (SWP) are applied for calculating steady-state operation modes (SSOM) and EMTP. Impedance loads can be defined in PC as those of AEM and SEM, as well as the static load (either unchanged impedance resistance $Z_{load}= R+jX$ or static load characteristics, SLC). The specificity of SLC in EMTP and SSOM calculations is that the SLCs defined for SOM are related to the entire load of particular nod, while in EMTP calculations they apply to only the static portion of loads (applicable to the entire load of a nod provided that there is no AEM and SEM, in this nod). In EMTP calculations Z_{load} = const is assumed as the default option.

Taking into consideration the large amount of initial data related to 0 kV to 220 kV networks, industrial load can be represented in form of SLC – $P_L(U, f)$, $Q_L(U, f)$, in EMTP calculations, for systemically important networks (330 kV and higher), similarly to SSOM calculations. It is acceptable since SCs in systemically important networks under consideration are electrically separated from the motor-type loads. Such SCs may affect these loads only in diminished and smoothed-out forms owing to the influence of power stations, reactive power compensation equipment, OHL resistances, power transformers, etc.

However, in a general case, substitution of dynamic load models by SLC, in EMTP calculations for distribution networks containing SPVSs and WPSs, as well as for industrial loads, in energy systems and isolated energy areas, would be not really correct.

The role of various AEM loads modeling methods in respect to EMTP parameters can be evaluated by comparing dependences $P_{load}(t)$ and $Q_{load}(t)$ shown in Fig. 2 where d_{AEM} is the share of AEM loads in particular energy area. These graphs correspond to three-phase SC, in distributionoĭ network, for three modeling load methods, for $Q_{load.0} = 0.5P_{load.0}$ (gray shading indicates the areas where method 1 differs from methods 2 and 3):

- method 1: $d_{AEM} = 0.7$, parameters AEM are averaged, simplified AEM model in form of the static asynchronous response,
- method 2: $d_{AEM} = 0$, load is represented by SLC;
- method 3: $d_{AEM} = 0$, Z_{load} =const.

Load modeling methods are represented in the descending order of their structural complicity. The more correct is the model the greater number of technical parameters from manufacturer has to be obtained since the datasheet specifications or reference data related to the corresponding AEMs and SEMs may be not enough.

From the analysis of Fig. 2 the conclusion can be made that curves $P_{load}(t)$ and $Q_{load}(t)$ are qualitatively identical, for all EMTP calculations, but certain quantitative differences depending on AEM parameters take place.

The principal distinctive feature of dependences $P_{load}(t)$ and $Q_{load}(t)$ corresponding to more accurate AEM models is that the transient processes do not coincide in time, for various AEM groups. Therefore, automatic starting will

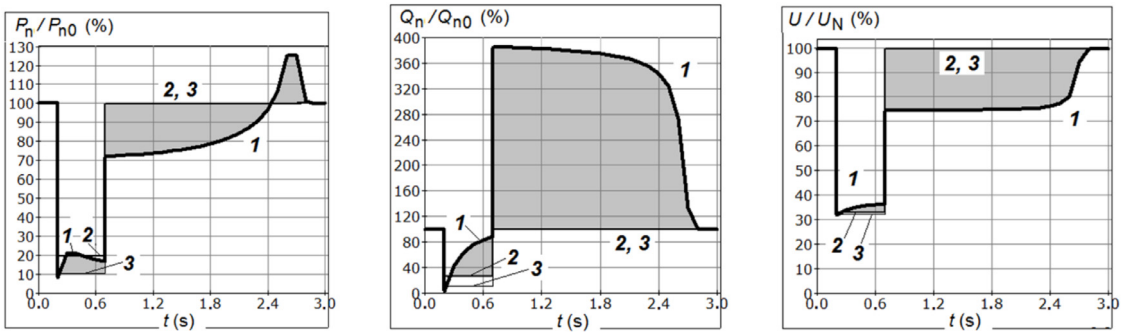

Fig. 2. Dependence of EMTP parameters during three-phase SC, in energy area, for tree load modeling methods.

finish at different moments depending on the AEM capacity use rate and the types of driven gear, for different AEM groups. That is why the reduction of additional reactive power consumption will be seen on the diagrams proceeding by several steps, in the course of AEM acceleration. Besides, a number of active power surges will take place in the process of AEM returning to its normal slip values.

It has to be noted that EMTP in AEM do not principally differ from SLC provided that the voltage on the terminals of AEM does not decrease fast and does not fall below its critical value (U_{cr}). This condition can only be fulfilled for SC occurring in an external distribution network, at a long distance from electric motors, or in industrial energy area, as well as when dynamic compensators of interruptions/undervoltages on AEM terminals are used.

If EMTP calculation results show that the voltagee on the terminals of AEM and SEM falls below U_{cr} it is not correct to represent nods of load with the help of generalized SLCs. In this case, the network of industrial energy area has to be introduced into the calculation model in its either complete or simplified form (reduction of the network elements may be allowed), by modeling the major electric power plants of this energy area including SPVSs and WPSs, nods of loads (with the application of dynamic models of major AEMs and SEMs), OHL and power transformers (Mitra et al. 2016 [29]; Kakran and Chanana, 2018 [30]).

In EMTP calculations, load impedance modeling method, for particular schematic and load-related conditions, has to be selected with the account of the test calculations results. Comparative calculations have to be performed with the use of the detailed and simplified load models. In case that the difference is not considerable, simplified models are preferable since designing complete models of load requires high labor costs.

As far as the reliable operation of the SPVS or WPS depends on the proper choice of the load description method, particular attention has to be payed to the problem of defining critical voltage on the AEM and SEM terminals.

3. Results and discussion

3.1. Defining critical voltage on the terminals of AEM and SEM

Critical voltage U_{cr} is the lowest voltage of the electric receiver static stability range. In reference to AEM and SEM, the process of static stability disturbance is called ‘changeover’ which means that electric motor cannot develop the required capacity shaft output and decelerates consuming greater reactive current and power from the network.

In real conditions, undervoltage on the terminals of many types of electric receivers causes their shutdown which has nothing in common with the disturbance of static stability. In industrial energy areas, shutdown of such electric receivers designed for voltages of 0.4 kV as fluorescent lamps may happen due to the self-tripping of magnetic starters (MS), undervoltage protection, etc.

In the new-type MSs, the self-tripping voltage range is 0.6 U_N to 0.7 U_N, while those that have been in operation for a long time have the self-tripping point on the level of 0.8 U_N to 0.9 U_N. MSs are activated due to the cascade tripping. For instance, switching-off single MS of oil pump maintaining pressure in AEM (SEM) bearing assemblies leads to activating the technological protection system, as the response to low oil pressure, in the lubrication circuit, and the corresponding motor stops. This technological process breaks resulting in disturbances at the industrial enterprise and switching-off other electric receivers by the system of technological interlocks. Such processes are

physically nonhomogeneous but all of them are followed by disturbing normal operation of electric consumers and damage. That is why it is advisable to apply parameter U_{cr} to all kinds of electric receivers malfunctioning due to the low voltage levels.

Value U_{cr} on the electric motor terminals can be calculated. Rotational moment produced by AEM under voltage U to $M = M_{max}(U/U_N)^2$ where M_{max} is the maximum rotational moment under voltage U_N. Making no account of insignificant effects, AEM has to develop rotating moment M_{op}, in normal operation mode, in which case the expression for critical conditions has the following form:

$$M_{max}\left(\frac{U_{cr}}{U_N}\right)^2 \approx M_{op} \tag{1}$$

Formula for calculating U_{cr} can be deduced from Eq. (1):

$$U_{cr} = U_N\sqrt{\frac{M_{op}}{M_{max}}} \tag{2}$$

The ratio of the operating moment to its nominal value approximately equals to capacity use rate k_{use} calculated as P/P_N. The ratio of M_{max} to M_N is the multipleness of maximum moment m_{max}. After transforming Eq. (2) we will have the following new expression for U_{cr}:

$$U_{cr} = U_N\sqrt{\frac{k_{use}}{m_{max}}} \tag{3}$$

Therefore, U_{cr} for AEM depends mainly on its capacity use rate. For the rated value of capacity use ($k_{use} = 1$) and $m_{max} = 2.2$ we obtain $U_{cr} = 0.675\ U_N$

Value U_{cr} for SEM also depends on loading but, in still greater degree, it depends on the value of excitation current (I_{ex}). If I_{ex} of SEM is maintained on one and the same level, for variable voltage, U_{cr} is defined by the preset operating value of the power factor ($\cos\varphi_{op}$). Higher values of I_{ex} correspond to reactive power output into the network, while its lower values correspond to consuming reactive power from the network. In the latter case, values U_{cr} will be high enough to initiate SEM changeover even in conditions of distant SCs, in an external network.

In case that undervoltage on the SEM terminals causes the growth of I_{ex}, as a result of automatic regulator (AER) activation or due to the step-wise boost, U_{cr} values for this SEM will be nearly identical to those of AEM and even lower. Such operating mode of SEM is the most preferable.

Cases are known when cos φ_{op} of SEM was retained on a level close to 1 in spite that its AER was out of operation. The optimal SEM operating mode is as follows: the stator current is as low as possible ($Q \approx 0$), I_{ex} is substantially lower than its rated value in which case SEM is heated insignificantly. It has to be noted that, in undervoltage conditions in the network, the steady-state stability of SEM will be disturbed before the step-wise excitation forcing with 0.8 U_N to 0.85 U_N actuation setpoint activates.

Value U_{cr} on the terminals of SEM group, for constant excitation currents, can be calculated as follows:

$$U_{cr} \approx U_N\, q^{-0.5} \tag{4}$$

where

$$q = 1 + \frac{1}{p^2}\left(\frac{U_N^2}{X} - Q\right)^2 \tag{5}$$

$$X = x_d \cdot \frac{U_N^2 \cos\varphi_N}{P_N} \tag{6}$$

and U_N is rated voltage of SEM (kV), P and Q are, respectively, active and reactive power consumed by the entire SEM group (MWM, MVAr), x_d is synchronous resistance (a.u.). $Q > 0$ when SEMs consume reactive power from the network.

Dependence U_{cr} on the operating value cos φ_{op} in accordance with Eq. (4) is shown in Fig. 3 (solid line).

If SEM has static-type excitation system (when I_{ex} is proportional to the voltage on SEM terminals) U_{cr} can be defined as follows, for the switched-off state of AER device:

$$U_{cr} \approx U_N\, q^{-0.25} \tag{7}$$

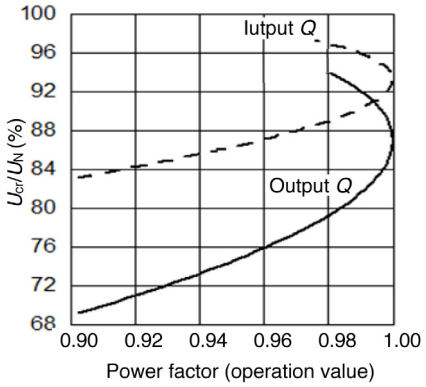

Fig. 3. Dependence $U_{cr}(\cos\varphi_{op})$ on the terminals of SEM type STD-5000-2.

Value q is calculated from Eq. (5), while dependence U_{cr} on the operating value of $\cos\varphi_{op}$ corresponds to the dashed line in Fig. 3. SEM stability will be high enough compared to the situation when value I_{ex} does not change, and value U_{cr} will be greater than the setpoint of excitation forcing activation.

Operating conditions in which SEM static stability is maintained with the use of excitation forcing cannot last for a long time because SEM will be switched-off by overcurrent protection leading to the disturbance of technological process. That is why the operating mode when $\cos\varphi_{op} \approx 1$ is strongly undesired, for SEM operating without voltage-controlled AER.

Values U_{cr}, in load nods of operating voltage 110 kV and higher, located away from electric receivers, may essentially exceed those of electric receivers since voltage loss in the network grows with decreasing voltage. In order to define adequate U_{cr} values, in the load nods, one has to extend the calculation algorithm with major OHLs and power transformers connecting particular load nods to the terminals of 6 kV to 10 kV electric receivers. The loads of 6 kV to 10 kV bars are allowed to be added together ignoring small resistance between them.

Values U_{cr} for AEM and SEM have to be defined according to their static stability conditions described by Eqs. (4)–(7). For other types of electric receivers, values $U_{cr} \approx 0.75U_N$, have to be assigned because they have self-disconnection function, for the reasons mentioned above.

SSOM calculations are performed in the conventional manner but with voltage control on the electric receivers' terminals. If, in any network nod, $U < U_{cr}$ this operating mode has to be qualified as failed to actually exist. Approximate values can be obtained in the assumption that, in nods 110 kV to 330 kV:

$$U_{cr} \approx \max(0.7U_N; 0.75U_N) \tag{8}$$

where U_{st} is voltage in particular load nod, in normal operating conditions of the energy system/isolated energy area.

Eq. (8) is not applicable to the following situations when U_{cr}may considerably exceed these specified values:

- there are long-distance heavily loaded OHLs connected to load nods, i.e. when voltage loss is rather high,
- step-down transformers are equipped with automatic voltage control (AVC),
- substantial share of active power (over 10 % to 15 %) is consumed by SEM group.

AVC device increases the voltage across electric receivers' terminals when that of mains falls which results in growth of the current consumed from the network. Therefore, the voltage loss in the supply mains grows thus reducing the voltage-related static stability reserve of the affected load nod.

In SSOM calculations, if $U < U_{cr}$, in one or several nods, the risk of both calculating process shutdown (due to its nonconvergence) and obtaining incorrect results is high. The latter may happen because AEMs and SEMs have not been taken into account that may easily changeover, as well as other electric receivers capable to switch-off spontaneously. Anyway, expressions for SLC make it possible to define P and Q for any voltage levels. This feature was purposely integrated into expressions for SLC. The matter is that in the iterative process of SSOM calculation, values of variables may change in a wide range. Therefore, iterative calculations would have not been possible if SLC were only applicable for $U > U_{cr}$.

That is why voltage levels control, in the nods of energy system/isolated energy area, has to be performed while calculating operating modes. It is expedient to extend the initial information related to the parameters of load nods by values U_{cr} and to check their compliance with condition $U > U_{cr}$, for all nods of the network section after successful completing iterations.

3.2. Adequate representation of SLC for voltage and frequency

An important difference between SLC calculations with the use of SSOM and EMTP is that SLCs defined in SSOM apply to the entire nod load while, in EMTP calculations, they determine only its static portion. In EMTP calculations, it is correct to apply SLC to the entire load provided that there is no AEM and SEM connected to this particular nod. Let us study the problem of adequate SLC representation for voltage and frequency, for operating mods calculations, in more detail.

Dependence of the active power on voltage is mainly defined by the configuration of electric receivers, and to a lesser extent it depends on the power loss. For static-type electric receivers, active power is defined as follows:

$$P_{stat} \approx \sum \frac{U^2}{R} \tag{9}$$

where R is active resistance.

When R does not depend (or scarcely depends) on voltage P_{stat} varies by 2% per 1% of voltage variation. If R decreases with voltage becoming smaller due to lower heating by flowing currents dependence of P_{stat} on voltage is weaker. Power consumption of incandescent electric lamps and fluorescent lamps decreases by ∼1.6% and 1% to 2% when voltage fall by 1%. Reactive power Q_{stat} consumed by static-type electric receivers is not normally high. Therefore, it can be ignored in a qualitative analysis.

In case of AEM and SEM, the major part of the active power consumed from the network is transferred to the rotating mechanisms (P_{mech}). Value P_{mech} is defined by the following expression:

$$P_{mech} = \omega_{mech} \cdot M_{mech}(\omega_{mech}) \tag{10}$$

where ω_{mech} is rotation velocity, M_{mech} is load resistant torque developed by rotating mechanism depending on ω_{mech}.

Value ω_{mech}, for SEM, depends only on the frequency until $U > U_{cr}$. For AEM, a slight dependence of ω_{mech} on voltage takes place due to the variation of AEM rotor slip in relation to the stator magnetic field. Correspondently, ω_{mech} varies, in a narrow range.

Active power loss in SEM and AEM, as wells that in mains OHL, are proportional to I^2 growing with the voltage decrease. And contrariwise, active power loss defined by excitation currents of SEM, AEM and power transformers decreases considerably with falling voltage. Consequently, active power consumed by electric motors weakly depends on voltage in which case derivative dP_{dv}/dU may have either positive or negative value.

Reactive power consumption by AEM decreases with voltage reduction due to that of excitation current, for normal voltage levels and overvoltages. Consumption of reactive power by AEM grows as a result of increasing current and $\Sigma I^2 X$ power loss, in undervoltage conditions, when voltage tends to U_{cr}. (An example of AEM SLC is shown in Fig. 4a).

Static characteristics for SEM active power are nearly similar to those of AEM. To a certain extent it applies to SEM reactive power characteristics, having in mind that Q_{SEM} consumption from the network grows when voltage tends to U_{cr}. However, SLC of Q_{SEM} is shifted towards the range of negative values if SEM transfers reactive power into the network (see Fig. 4b). Fig. 4b presents SLC of SEM, for switched-on and switched-off AER due to the voltage deviation, for various cos φ values.

Arrows indicate critical operating conditions. For all electric receivers, positive values of active/reactive power correspond to power consumption from the network.

It is seen from Fig. 4b that SEM starts to consume reactive power from the network, in undervoltage conditions, if AER is shut-off, while for the switched-on AER generation of reactive power grows with voltage.

The most commonly applied SLC is that in which active and reactive power consumed in a particular nod, in the initial operating mode (P_{n0}, Q_{n0}), are introduced not in SLC polynomial but with the help of separate multiplier.

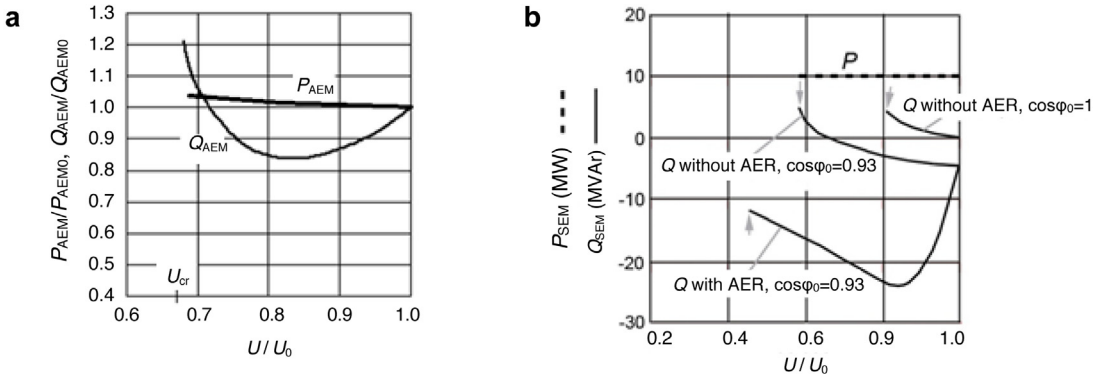

Fig. 4. (a) SLC for AEM, in conditions of rated loading and small resistance between AEM and power source, (b) SLC of SEM, for switched-on and switched-off AER due to the voltage deviation, for various cos φ values.

It makes it possible to apply the same SLCs to different nods having similar load impedance but different P_{n0} and Q_{n0} values. SLC polynomials (functions φ_1 and φ_2) are dimensionless:

$$\frac{P_n}{P_{n0}} = \varphi_1\left(\frac{U}{U_0}, \frac{f}{f_N}\right)$$
$$\frac{Q_n}{Q_{n0}} = \varphi_2\left(\frac{U}{U_0}, \frac{f}{f_N}\right) \quad (11)$$

$$\text{i.e.} \quad P_n = P_{n0} \cdot \varphi_1\left(\frac{U}{U_0}, \frac{f}{f_N}\right)$$
$$Q_n = Q_{n0} \cdot \varphi_2\left(\frac{U}{U_0}, \frac{f}{f_N}\right) \quad (12)$$

By transition to dimensionless SLCs, with the use of Eqs. (11) and (12), the process of their representation for modeling becomes much easier. Nevertheless, it is not convenient for $Q_{n0} < 0$ which belongs to possible options, in case of large-capacity devices application designed for reactive power compensation, in the circuit of internal power supply of industrial energy areas.

Variations of the consumed active power due to frequency change is negligible, for static-type electric receivers. For AEM and SEM, values of net capacitance P_{mech} transferred to the rotating mechanism is defined by Eq. (10). Dependences of load resistant torque M_{mech}, for the driven mechanism, on angular rate ω_{mech} differ, for various mechanisms. Correspondently, dependences P_{mech} (ω_{mech}) are not identical as it is shown in Fig. 5 where M_{mech} (ω_{mech}) are drawn with dashed lines while P_{mech} (ω_{mech}) are drawn with solid ones.

Since angular rate ω_{mech} is proportional to the mains frequency, within the accuracy of AEM slip variations, while the power of a driven mechanism is proportional to the active power consumed from the network, with an accuracy to the value of power loss, SLCs of AEM and SEM correspond to the solid lines, in Fig. 5.

Dependences $Q_n(f)$ are defined by the same factors as dependences $Q_n(U)$. Besides, it has to be kept in mind that inductive reactances are proportional to frequency. Therefore, reactive power loss in the network ($\Sigma\, I^2X$) decreases while this of excitation currents ($\Sigma U^2/X_\mu$) grows with frequency reduction.

In distribution networks of energy areas with small-distance OHL and voltage nods whose voltage is close to U_N the aggregate loss associated with excitation currents of AEM, SEM and power transformers exceed those of OHL series resistance. That is why the combined effect of small frequency drops appears in P_n reduction and Q_n growth.

Results of general analysis and field experiments show that processes (fast, long-duration) take place, in the impedance load, due to the voltage and/or frequency variations in mains. These processes make their effect on the power consumption. There exist two principally different types of such processes and reasons for their activation:

1. Voltage variations in energy areas where loads are represented by their SLCs, in calculation model, that are initiated due to the activation of AVC devices controlling transformer ratios, in substations, as well as a result of slower manual control of switching equipment on live power circuits.

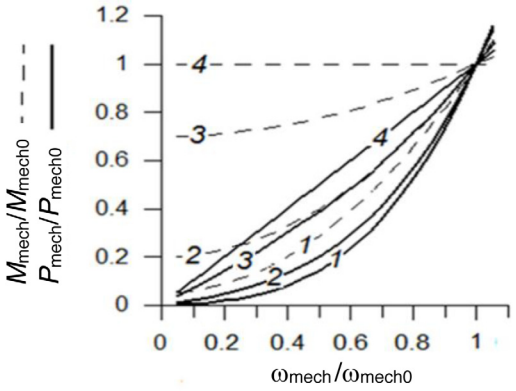

Fig. 5. Dependences M_{mech} (ω_{mech}) and P_{mechx} (ω_{mech}): *1* – radial flow compressor, *2* – hydraulic pump with low static head, *3* – hydraulic pump with high static head, *4* – reciprocating compressor or grinder.

2. Change of the number of electric receivers in active state in accordance with the technological process conditions. Example: drying processes for raw materials, active mineral supplements and solid fuels used for cement manufacture extend in time, in undervoltage conditions. In such cases, the need for greater number of active air blowers may arise, in systems where a certain pressure level of the working medium shall be maintained. When undervoltage on the AEM terminals occurs the performance of pumps decreases, and the automated control system (ACS) issues control signal for starting more backup pumps, in order to restore the required pressure level, in the system.

The effects described above have to be explained as an adaptation of consumers to the changing energy supply environment. The distribution of these phenomena in time depends on characteristics of particular impedance load.

For inertia-free (such as thyristor-controlled circuitries applied in DC driving system) or fast-response (for instance, tractive effort control systems used in electric transport enterprises) ACS operating mode, these processes cannot be detected against the background of standard reactions of electric receivers to the power supply mode variations. In these cases, natural SLCs defining instant reactions of P_{load} and Q_{load} to the voltage and/or frequency deviations in the network will be obtained, in the experimental processe.

Slow response of electric receivers to the network operating parameters deviation has to be qualified as consumer adaptation. The SLC form, with the account of adaptation processes, is shown in Fig. 6 where voltage is controlled manually, between points 1 and 2, while between points 2 and 7, load adaptation to these changes takes place. In calculations, particularly this form of SLC has to be considered in case when operating modes that require certain time intervals (for instance, from 10 minutes to 1 h) for coming to stay at their steady-state level are dealt with. For

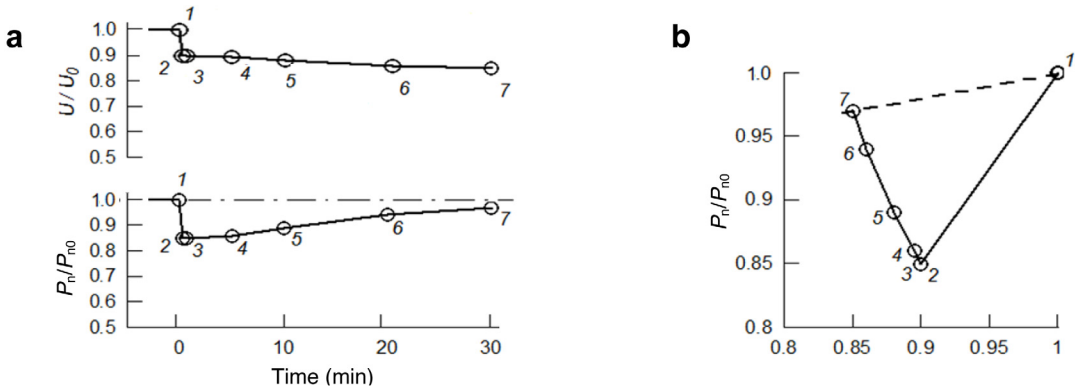

Fig. 6. Time diagram of P_{load} depending on the change of mains voltage: (a) example of natural SLC behavior (interval between points 1 and 2), (b) SLC with the adaptation effect (interval between points 1 and 7).

longer time intervals, cause–effect relationships between the power consumption and network operating parameters lose their dependability due to the stochastic non-regular character of load oscillations.

Graphs in Fig. 6 show that when mains undervoltage occurs values P_{load} and Q_{load} decrease initially but then they start growing making the post-emergency operation mode heavier. That is why load impedance adaptation effects have to be considered while calculating post-emergency operation conditions since they may cause disconnecting SPVSs and WPSs.

3.3. Specific aspects of calculating EMTP for asynchronous motors

In order to raise the accuracy of EMTP calculation results for power networks in industrial energy areas comprising AEMs, for all values of rotation velocity, dependence of rotor resistances x and r on the rotation velocity has to be taken into account.

Physical behavior of magnetic fields and currents in AEM rotor is such that the current flows within the rotor meet different resistance depending on the depth of their location. In Fig. 7a, simplified schematic view of AEM cross-section portion where lines of magnetic field force are shown, for two current branches, one of which is located in the depth of the rotor and the other flows in its subsurface area. It is seen that power lines of subsurface currents close in the air gap thus reducing the aggregate strength of magnetic field.

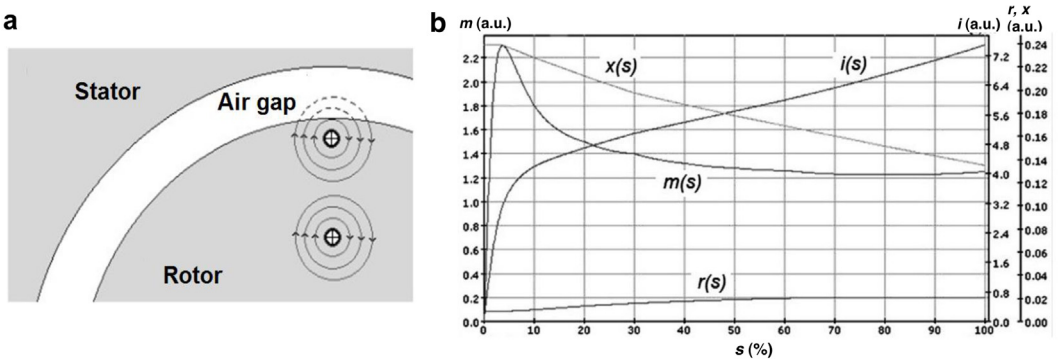

Fig. 7. (a) simplified schematic view of AEM cross-section, (b) dependence of AEM parameters on motor slip (s).

Until the value of AEM rotation velocity is high the frequency of currents in the rotor is low, and the difference between inductance values in the depth and on the surface of the rotor is insignificant. However, decreasing rotation velocity leads to the growth of frequency of currents, in rotor, and the currents flowing in the depth of rotor meet much greater resistance compared to those flowing in the subsurface. Therefore, the effect of current flows ejection towards the surface of the rotor occurs.

The average inductance value decreases as long as the currents are ejected towards the surface since a certain portion of magnetic field generated by rotor currents closes in the air gap, while the active resistance grows because of the cross-section reduction through which these currents flow. Examples of $x(s)$ and $r(s)$ dependences defined by rotor currents ejection are shown in Fig. 7b.

Methods are known that make it possible to take account of resistance change, in AEM rotor, for various slip values, and to obtain sufficiently correct representations for $M(s)$ and $I(s)$ characteristics. These characteristics have to be defined for U_N.

In the first method, the parallel current routes, in the rotor, are separated one from another in order to describe them with the use of multi-loop structure composed of a number of parallel current branches. Such model will be adequate provided that sufficient number of parallel circuits has been selected and that their parameters have been correctly defined. However, selecting resistance values is not unique even for only two circuits, in the rotor schematic model.

This method is applied in SWP ‘EUROSTAG’ implementing ‘complete model’ in which AEM equivalent-circuit resistances correspond to the defined AEM parameters (M and I), for two slip values. Critical slip s_{cr} is defined for rotation speed close to its rated value when motor torque attains its maximum. The second value has to be specified

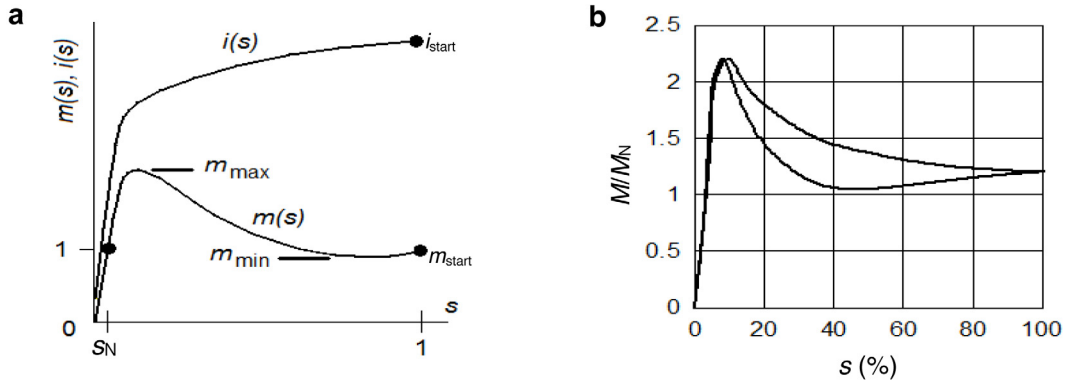

Fig. 8. (a) Graphs of initial data for modeling $m(s)$ and $i(s)$ in AEM, (b) Dependence of electromagnetic moment m on AEM slip s.

for zero rotation speed. Selection of reference resistances is rather correct. Nevertheless, one has to check whether it complies with the intergraduated values m and i for $s > s_{cr}$ (see Fig. 8a). Values of m_{max} and m_{min} are not normally associated with particular values of s.

The advantage of AEM model in SWP 'EUROSTAG' is that it takes the account of transient electromagnetic processes, in rotor, like those of synchronous mechanisms. In this EMTP model, AEM motor torque depends not only on s but also on derivative ds/dt (see Fig. 8b). Graphs in Fig. 8b were calculated for the following conditions: $M_{max}/MN = 2.2$, $M_{start}/MN = 1.2$.

Among disadvantages of such AEM model the complicity of parameter definition for two circuits of the rotor schematics has to be mentioned. The problem is that there exist many variants while dependences $M(s)$ and $I(s)$ on circuit resistances are non-linear. Moreover, there is no support algorithm, in SWP 'EUROSTAG', making it possible to define the desired parameters for either automated or semi-automated operating mode. That is why application of double-circuit AEM rotor model is not effective, in real conditions.

The second method for sampling correct values of $x(s)$ and $r(s)$, for AEM, is to define slip values by calculations. SWP 'MUSTANG' comprises a subroutine making it possible to specify relative values $m = M/M_N$, $I = I/I_N$, for any slips, in order to control the shape of graphs $m(s)$, $i(s)$, $x(s)$ and $r(s)$. Certain calculating instruments for compensating possible nonmonotonicity of $i(s)$, $x(s)$ and $r(s)$ variations (which is an indicator of some errors) is also provided.

Let us describe the algorithm of operations designed to obtain desired results:

- specifying catalogued data for particular AEM,
- values of x and r are calculated in SWP, for AEM equivalent-circuit, in which case intergraduated values of $x(s)$ and $r(s)$ are determined by linear interpolation in resistance and non-linear interpolation in motor torque and current,
- dependences $m(s)$ and $i(s)$ are calculated in SWP and are represented in graphic form,
- either parameters of AEM calculation model have to be checked or intergraduated values of $m(s)$ and $i(s)$ have to be introduced to adjust the model. It is necessary in case that either minimal motor torque m_{min} exceeds it actual value or dependence $i(s)$ appears to have non-monotonous form,
- recalculation of $x(s)$, $r(s)$, $m(s)$ and $i(s)$ is carried out, in SWP, and calculation results (see Fig. 7b) that can be corrected again are represented in graphic form.

As a rule, simplified AEM models describe EMTP correctly enough (AEM decelerating in undervoltage conditions, the processes of AEM automatic starting) but ignoring electromagnetic processes has the following consequences:

1. Voltage across AEM terminals decays during a time period from tenths of a second to several seconds after its disconnecting from mains line. It is important to bear in mind in terms of selecting setpoints for automatic starting devices of the energy system. It has to be noted that, in simplified models, voltage across AEM terminals falls down to zero immediately.

2. Graphic diagrams for AEM current and power after switching-over comprise variable components that are not taken account of, in simplified AEM model, which has to be considered wile analyzing operation of PR equipment in SPVSs, WPSs and other PGPs.

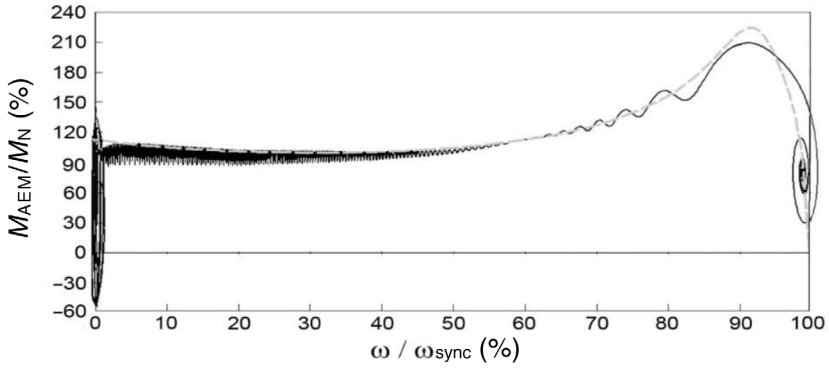

Fig. 9. Calculated asynchronous characteristics of AEM.

Input power of AEM depends on not only motor slip *s* but also on its derivative *ds/dt*. That is why AEM asynchronous characteristic gets distorted when it starts from a constant-voltage power supply. Fig. 9 shows AEM asynchronous characteristic in witch electromagnetic processes in rotor have been taken into account (solid line), as well as its static asynchronous characteristic (gray dashed line).

When necessary, specific issues related to the simplified AEM model that we have discussed can be taken into consideration, in EMTP calculations with the use of AEM 'complete model' with the application of SWP 'EUROSTAG'. The use of SWP 'MUSTANG' will require building an AEM model that takes account of the electromagnetic processes in rotor in which case modeling has to be supported by the initial SEM model.

In EMTP calculations, an adequate account of the impedance load, as a whole, and particularly that of AEM characteristics, enables to evaluate the effect of emergency disturbances on the operating mode parameters, in industrial energy areas. This provides the opportunities for taking well-founded technical decisions, while preparing design projects, making it possible to prevent mass-scale outages of SPVSs, WPSs and other PGP thus contributing to a more reliable energy supply.

4. Conclusion

The influence of the impedance load on the parameters of electromechanical transient processes, in industrial energy areas, is significant. Incorrect account of the load characteristics, in the design process, leads to mass-scale outages of SPVSs, WPSs and other generating facilities due to emergency disturbances and therefore, causes considerable damage because of interruption of energy supply to electric receivers.

Alarm processes characterized by active power deficit, in both island and isolated operating modes, develop in an essentially heavier form, for SPVSs and WPSs, other generating plants and electric receivers that have not been disconnected compared to their operation in parallel with the energy system.

An approach to selecting methods for impedance load modeling, in industrial energy areas, and those for defining the value of critical voltage across the load terminals have been suggested. The reasonability of electric motor dynamic models application has been substantiated.

Specific application conditions of impedance load static characteristics in voltage and frequency, in electromechanical transient processes calculations, have been studied and examples when it is acceptable have been discussed.

Taking into account specific features of various software packages for operating modes calculations in relation to the electric motors behavior modeling makes it possible to adequately describe them as a part of the entire impedance load. Methods for taking into account electromagnetic transient processes, in rotors of asynchronous motors, have been described.

Adequate account of the impedance load ensures reliable functioning of SPVSs and WPSs as a part of energy systems and isolated energy areas thus preventing their unreasonable outages and breakages of power supply to electric receivers, in industrial enterprises.

Declaration of competing interest

The authors declare that they have no known competing financial interests or personal relationships that could have appeared to influence the work reported in this paper.

Data availability

No data was used for the research described in the article.

Acknowledgments

This work is supported by the Russian Science Foundation under grant 21-79-30013 in the Energy Research Institute of the Russian Academy of Sciences.

References

[1] Zeng B, Wen J, Shi J, Zhang J, Zhang Y. A multi-level approach to active distribution system planning for efficient renewable energy harvesting in a deregulated environment. Energy 2016;96:614–24. http://dx.doi.org/10.1016/J.ENERGY.2015.12.070, 2016.

[2] Eroshenko SA, Samoylenko VO, Pazderin AV. Renewable energy sources for perspective industrial clusters development. In: Proc. of the 2nd int. conf. on industrial engineering, applications and manufacturing. 2016, p. 1–5. http://dx.doi.org/10.1109/ICIEAM.2016.7911460, 2016.

[3] Izmailov AYu, Lobachevsky YaP, Shepovalova OV. Complex energy supply systems for individual sites. Energy Procedia 2019;157:1445–55. http://dx.doi.org/10.1016/J.EGYPRO.2018.11.309.

[4] Buchholz BM, Styczynski Z. Smart grids – fundamentals and technologies in electricity networks. New York: Springer Heidelberg; 2014.

[5] Papkov B, Gerhards J, Mahnitko A. System problems of power supply reliability analysis formalization. In: Proc. of the 2015 ieee 5th int. conf. on power engineering, energy and electrical drives. 2015, p. 225–8. http://dx.doi.org/10.1109/POWERENG.2015.7266324, 2015.

[6] Ilyushin PV, Shepovalova OV, Filippov SP, Nekrasov AA. Calculating the sequence of stationary modes in power distribution networks of Russia for wide-scale integration of renewable energy-based installations. Energy Rep 2021;7:308–27. http://dx.doi.org/10.1016/j.egyr.2021.07.118, 2021.

[7] Rylov AV, Ilyushin PV, Kulikov AL, Suslov KV. Testing photovoltaic power plants for participation in general primary frequency control under various topology and operating conditions. Energies 2021;14(16):5179. http://dx.doi.org/10.3390/en14165179, 2021.

[8] Zimba SK, Nyamutswa I, Chikova A. Islanding power systems to minimize impact of system disturbances in southern African power pool. In: Proc. of the 2017 IEEE AFRICON. 2017, p. 1107–12. http://dx.doi.org/10.1109/afrcon.2017.8095637, 2017.

[9] Singh M, Meera KS, Joshi P, Prakash P. Islanding scheme for power transmission utilities. In: Proc. of the 6th int. conf. on computer applications IN electrical engineering-recent advances. 2017, p. 69–73. http://dx.doi.org/10.1109/CERA.2017.8343303, 2017.

[10] Ilyushin PV, Kulikov AL, Suslov KV, Filippov SP. Consideration of distinguishing design features of gas-turbine and gas-reciprocating units in design of emergency control systems. Machines 2021;9(3):47. http://dx.doi.org/10.3390/MACHINES9030047, 2021.

[11] Shepovalova OV. Mandatory characteristics and parameters of photoelectric systems, arrays and modules and methods of their determining. Energy Procedia 2019;157:1434–44. http://dx.doi.org/10.1016/j.egypro.2018.11.308, 2019.

[12] Shepovalova OV, Belenov AT. Investigation of DC motors mechanical characteristics with powered by comparable capacity PV array. Energy Procedia 2017;119:990–4. http://dx.doi.org/10.1016/j.egypro.2017.07.132, 2017.

[13] Strebkov DS, Shepovalova OV, Bobovnikov NI. Investigation of high-voltage silicon solar modules. In: AIP conf.proc, Vol. 2123. 2019, 020103. http://dx.doi.org/10.1063/1.5117030, 2019.

[14] Khimenko AV, Prantsuz OS, Glebova IA, Ponomarev AK. Evaluation of the efficiency of heat storage by a solid-state electric thermal storage. J Phys Conf Ser 2020;1560:012049. http://dx.doi.org/10.1088/1742-6596/1560/1/012049, 2020.

[15] Li Z, Yao G, Geng G, Jiang Q. An efficient optimal control method for open-loop transient stability emergency control. IEEE Trans Power Syst 2017;32(4):2704–13. http://dx.doi.org/10.1109/TPWRS.2016.2629620, 2017.

[16] Tina GM, Licciardello S, Stefanelli D. Conventional techniques for improving emergency control of transient stability in renewable-based power systems. In: Proc. of the 9th int. Renewable energy congress (IREC 2018), 2018, p. 1–6. http://dx.doi.org/10.1109/IREC.2018.8362545, 2018.

[17] Eroshenko SA, Ilyushin PV. Features of implementing multi-parameter islanding protection in power districts with distributed generation units. In: Proc. of 2018 IEEE 59th int. scientific conf. on power and electrical engineering of riga technical university. 2018, p. 1–6. http://dx.doi.org/10.1109/RTUCON.2018.8659857, 2018.

[18] Ufa RA, Rudnik VE, Malkova YY, Bay YD, Kosmynina NM. Impact of renewable generation unit on stability of power systems. Int J Hydrogen Energy 2022;47(46):19947–54. http://dx.doi.org/10.20221016/j.ijhydene.2022.04.141.

[19] Gurevich YuE, Libova LE. Application of mathematical models of electrical load in calculation of the power systems stability and reliability of power supply to industrial enterprises. Moscow: ELEKS-KM; 2008.

[20] Gurevich YuE, Kabikov KV. Features of power supply, focused on the uninterrupted operation of industrial consumers. Moscow: ELEKS-KM; 2005.

[21] Mokryani G, Hu Y, Pillai P, Rajamani H-S. Active distribution networks planning with high penetration of wind power. Renew Energy 2017;104:40–9. http://dx.doi.org/10.1016/J.RENENE.2016.12.007, 2017.
[22] Shushpanov I, Suslov K, Ilyushin P, Sidorov D. Towards the flexible distribution networks design using the reliability performance metric. Energies 2021;14(19):6193. http://dx.doi.org/10.3390/en14169854, 2021.
[23] Gurevich YuE, Libova LE, Okin AA. Calculations of stability and emergency automation in power systems. Moscow: Energoatomizdat; 1990.
[24] Raza S, Arof H, Mokhlis H, Mohamad H, Illias HA. Passive islanding detection technique for synchronous generators based on performance ranking of different passive parameters. IET Gener Transm Distribution 2017;11:4175–83. http://dx.doi.org/10.1049/iet-gtd.2016.0806, 2017.
[25] Ruchika Gupta P, Jain DK, Bhatia RS. Islanding detection technique for a distributed generation with perfectly matched load condition. In: Proc. of the 2017 int. conf. on computing, communication and automation. 2017, p. 1503–6. http://dx.doi.org/10.1109/CCAA.2017.8230038, 2017.
[26] Ramadan M, Hao E, Logenthiran T, Naayagi R, Woo W. Islanding detection of distributed generation in presence of fault events. In: Proc. of the TENCON 2017-2017 IEEE region 10 conf. 2017, p. 1919–24. http://dx.doi.org/10.1109/TENCON.2017.8228172, 2017.
[27] Singh V, Sharma J. A review on distributed generation planning. Renew Sustain Energy Rev 2017;76:529–44. http://dx.doi.org/10.1016/J.RSER.2017.03.034, 2017.
[28] Mehigan L, Deane JP, Gallachóir BPO, Bertsch V. A review of the role of distributed generation (DG) in future electricity systems. Energy 2018;163:822–36. http://dx.doi.org/10.1016/j.energy.2018.08.022, 2018.
[29] Mitra J, Vallem MR, Singh C. Optimal deployment of distributed generation using a reliability criterion. IEEE Trans Ind Appl 2016;52:1989–97. http://dx.doi.org/10.1109/tia.2016.2517067, 2016.
[30] Kakran S, Chanana S. Smart operations of smart grids integrated with distributed generation: a review. Renew Sustain Energy Rev 2018;81(1):524–35. http://dx.doi.org/10.1016/j.rser.2017.07.045.